Authors:

A biomimetic flapping based double-hull boat with vision-based target tracking capability

Fengran Xie, frxie@mae.cuhk.edu.hk, The Chinese University of Hong Kong
Yong Zhong, yzhong@mae.cuhk.edu.hk, The Chinese University of Hong Kong
Zheng Li, lizheng@cuhk.edu.hk, The Chinese University of Hong Kong
Ruxu Du, rdu@mae.cuhk.edu.hk, The Chinese University of Hong Kong

Keywords:
Flapping based Propeller, Wire-driven Mechanism, Vision, Target Tracking, Navigation, Biomimetic, Autonomous

DOI: 10.14733/cadconfP.2017.459-466

Introduction:

With millions of years of evolution, fish is an excellent swimmer having fast swimming speed, high efficiency and great maneuverability. In recent years, a large number of studies have been carried out on developing fish-like propellers, which are safer, of lower noise and more efficient than traditional rotary propellers. For example, Li *et al* [3] developed a wire-driven robot fish with a streamlined body and a flapping tail, which can perform various flapping motions for cruising and turning. Pablo *et al* [1] designed and fabricated a soft body robot fish. Yu *et al* [6] created a multi-joint robot fish. Though, a few has worked on the robot fish control issues, such as target tracking and collision avoidance.

On the other hand, 90% of the world's trade is carried by water transportation [2]. Target tracking and collision avoidance are essential on wharf management. There are however several difficulties for solving this problem. Firstly, underwater is such complex environment full of unpredictability. Waves, turbulence, ocean current may change anywhere anytime, which could have a big impact on motion of vessel in tracking targets and avoiding barriers. Secondly, powered by rotary propeller and steering by rudder, the aquatic vessel is a system with large hysteresis, whose braking distance is very longer. It is difficult to stop and turn sharply and reach specific positions. In comparison, it is well known that fishes can easily turn around with very small turning radius. This motivates researchers around the world to find a biomimetic solution. For example, Xie *et al* [5] used situated-behavior-based decentralized control to deal with target tracking and collision avoidance between multiple robot fish collaboration. Nevertheless, so far the achievements are rather limited.

In this paper, we present a wire-driven flapping based double-hull boat with a vision-based target tracking system. The boat has two identical wire-driven propellers mimicking fish flapping locomotion and yet providing large loading capacity. Various motions can be performed including cruising and turning with high stability. Moreover, the turning radius is only 180 mm (0.517 body length (BL)) and the turning speed is up to 13.9˚/s. A camera is mounted on the boat to capture the surrounding information. The image processing is executed by a microcontroller on board to identify the target position. Accordingly, the boat can change the flapping patterns to track the target by using the modeless method. Based on experimental testing, the boat can always track the target successfully. This research lays the foundation for autonomous navigation in the future.

Main Idea:

1. Design and modeling

The design of the fish-like double hulls boat is depicted in Fig. 1(a). It consists of two identical hulls connected by a deck in between. The control board, the battery and the camera are mounted on the deck. At the bottom of each hull, a wire-driven propeller is installed, which composes of 7 vertebrae and is driven by a servomotor. Fig. 1(b) shows the mechanism of the wire-driven propeller.

A pair of wire passes through the 7 vertebrae. One end of wire is fixed at the 7th vertebra and the other end of wire is fastened at the drum wheel. The drum wheel is connected to the servomotor directly. When the motor rotates back-and-forth, the wire-driven tail gives flapping motion and thus, generates the thrust for the boat. More details of the double-hull boat can be found in [4].

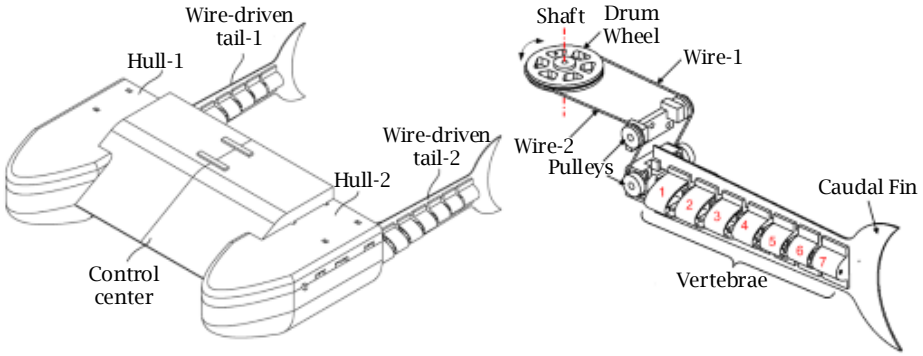

Fig. 1: Fish-like double hulls boat: (a) CAD model, (b) Mechanism of the wire-driven tail [4].

The thrust force of the wire-driven propeller can be descripted as follows:

$$F_t = \sum_{i=1}^{N} 0.5 C_l \rho A_i (\vec{v}_i \cdot \vec{v}_i) \cdot \sin\theta_i \tag{1}$$

where, C_l is the lift coefficient of the vertebrae; ρ is the water density; A_i is the flapping area; $\vec{v}_i$ is flapping velocity; θ_i is the flapping angle and subscript i = 1, 2, .., 7, is used to index the vertebrae. Assume the rotational angles of the vertebrae are the same, that is:

$$\theta_i = \frac{i}{N} \cdot \Theta \tag{2}$$

where, Θ is the flapping amplitude of the propeller. The position of each joint is given by

$$\begin{cases} x_i(t) = \sum_{j=1}^{i} \left(\left(H + h_0 \right) \cos\theta_i \right) \\ y_i(t) = \sum_{j=1}^{i} \left(\left(H + h_0 \right) \sin\theta_i \right) \end{cases} \tag{3}$$

where, $x_i(t)$ and $y_i(t)$ are the coordinates of the i^{th} joint the propeller; the length, H, of each vertebra is the same, and the gap, h_0, between the vertebrae is also the same. The flapping area of the vertebra i, A_i can be computed by

$$A_i = 2 \frac{y_i(t) - y_{i-1}(t)}{\sin\theta_i} \theta_i \tag{4}$$

From Eqs (1), (2), (3) and (4), it can be observed that the thrust of the propeller is linear related to the flapping area, and the flapping area is related to the flapping amplitude of the tail. Therefore, the thrust magnitude of each propeller can be controlled by adjusting the flapping amplitude Θ. Moreover, the turning of the double-hull boat can be controlled by changing the flapping amplitude of the propellers, as shown in Fig. 2. If $\Theta_{Left} < \Theta_{Right}$, the boat would turn to the left; if $\Theta_{Left} > \Theta_{Right}$, the boat would turn to the right.

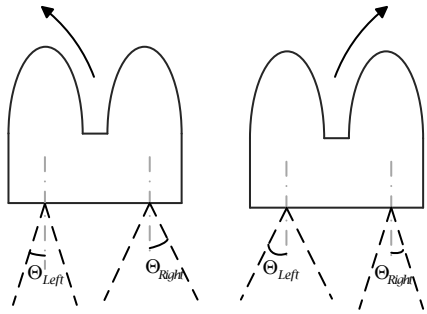

Fig. 2: Maneuvering: (a) Turn left $\Theta_{Left} < \Theta_{Right}$, (b) Turn right $\Theta_{Left} > \Theta_{Right}$

2. Cruising modes

There are two cruising modes for the double-hull boat, as shown in Fig.3. In cruising mode 1, two tails flap in the same direction. As a result of that, thrust force is supposed to be double. However, the lateral force will also be double, which may cause the boat sways from side to side. This is undesirable for cruising. The other cruising mode is that two tails flap in the opposite direction. In this scenario, the thrust force is also double and the lateral force of hulls would be cancelled out. Moreover, a water jet is generated when the two propellers flap inward, which would yield additional thrust. Thus, cruising mode 2 is more stable and more efficient, which will be adopted in the following experiments.

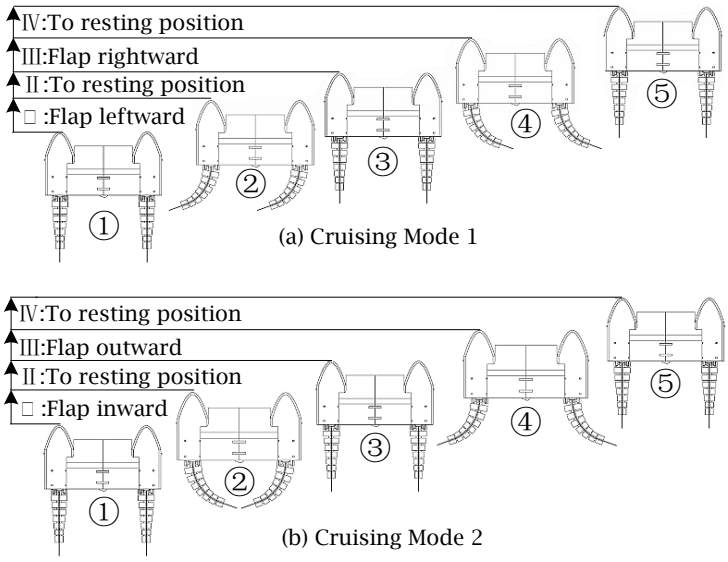

Fig. 3: Cruising Mode: (a) Flap in the same direction, (b) Flap in the opposite direction [4].

3. Turning modes

Turing performance, including turning radius and turning speed, is one of the key characteristics in boat maneuvering and parking in the harbor. There are three turning modes for the double-hull boat, as shown in Fig. 4. Let us assume the boat to maneuver leftward for better illustration. In tuning mode 1, the two tails flap leftward, and then to the resting position, synchronously. In turning mode 2, one tail works as a rudder, in the leftmost position for a whole turning cycle, while the other tail flaps leftward and then to the resting position. In turning mode 3, which is similar with turning mode 2, one tail also works as a rudder, while the other one flaps between leftward and rightward continuously.

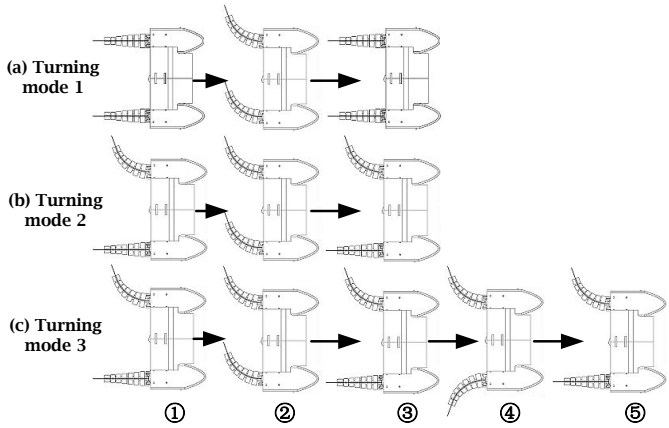

Fig. 4: Turing modes.

4. Imaging and image processing

The image acquisition and processing system includes a smart camera, an image processing unit and a real-time control system. This system can acquire images (640×480 pixels) continuously and calculate the center of target position. The image processing process is shown in Fig.5, and each step is detailed as follows:

(a) Image acquisition: Acquire a 640×480 RGB image from the camera;
(b) Color plane extraction: Extract one of the three color planes (red, green, blue) from an image. This will convert a RGB image to a grayscale image;
(c) Threshold: Select pixels of certain range in the output grayscale image;
(d) Morphology: Perform operations on small blobs in binary image;
(e) Shape detection: For a circular part, find the center and radius of circular particles in an image.

Fig. 5: Steps of image processing.

Fig.6 shows a set of sample results: (a) the original RGB image; (b) the corresponding grey scale image; (c) the binary image (the threshold is set at 170); (d) the outcome of the eroding operation, which removes the shades and other noises (small blobs); (e) the identified center position and radius.

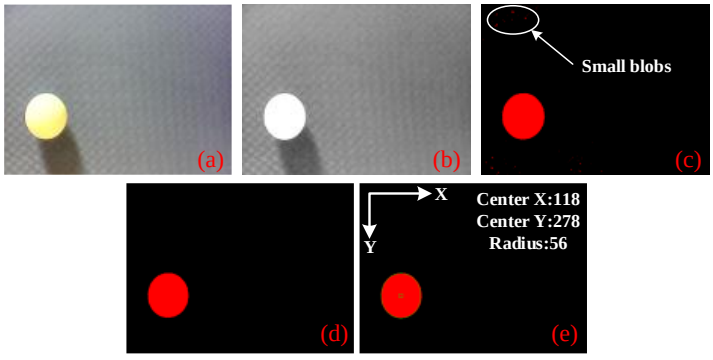

Fig. 6: A demonstration example: (a) the original image, (b) the black-and-white image, (c) the binary image, (d) the outcome of the eroding operation, (e) the detected circle.

5. The Modeless Control

Since it is difficult to precisely model the boat due to its large hysteresis and the complexity in the water, the modeless method is adopted to control the boat. In order to lead to the target, the target should be on the perpendicular bisector of the two hulls. In other words, the target should locate at the middle of the acquired image. Since the boat navigates on the surface of water, only X coordinate is taken into consideration. The size of image is 640×480, so the coordinate of middle of the X axis is 320. If center x of target is less than 320, the orientation of the boat should be modified to turn left, which means more driving force should be generated in the right motor. If center x of target is more than 320, the orientation of the boat should be modified to turn right, which means more driving force should be generated in the left motor. The difference between center x of target and middle x coordinate of image is used as a feedback signal to tune the oscillating amplitude of the propulsive tails as shown in Eqn. (5) and Eqn. (6).

To turn left,

$$\begin{aligned} A_{Left} &= A_0 \\ A_{Right} &= A_0 + K_P \left| X_t - X_{Mid} \right| \end{aligned} \tag{5}$$

To turn right,

$$\begin{aligned} A_{Right} &= A_0 \\ A_{Left} &= A_0 + K_P \left| X_t - X_{Mid} \right| \end{aligned} \tag{6}$$

From Eqs (5) and (6), A_{Left} , A_{Right} are the calculated flapping amplitudes of left and right propulsive tails; A_0 is the original flapping amplitude; K_p is the proportional coefficient; X_t is x coordinate of target; X_{Mid} = 320 is the X coordinate of the middle point in the acquired image.

6. Prototype and experiments

Fig. 7 shows the prototype of the boat with its control platform. A microcontroller (Xilinx Zynq-7010) with real-time system is used as the control board. The camera acquires image and sends to MCU. Two propulsive tails are driven by two servo motors, which are controlled by PWM signals. All data is sent back to a laptop for reference through a wifi module.

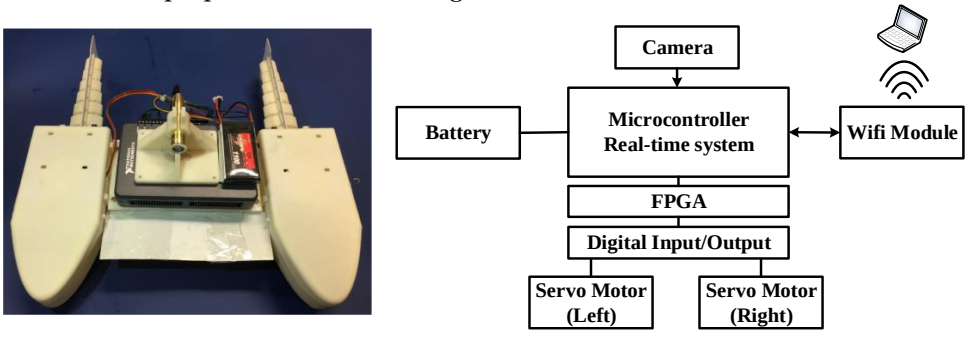

Fig. 7: The biomimetic flapping based double hulls boat: (a) Prototype, (b) Control platform.

The first experiment is to explore the cruising performance of the boat. As discussed in the previous section, cruising mode 2 is more stable and efficient and hence, is adopted. Two different flapping patterns are tested: sinusoidal and triangle. In both cases, the flapping frequency is 1 Hz and the flapping amplitude is 44°. The cruising distance is 880 mm. Time is counted after the speed of the boat has been stabilized. Fig.8 shows cruising time under the sinusoidal and triangle patterns are 8 seconds and 9.04 seconds, corresponding to 0.314 BL / second and 0.279 BL / second respectively. It is seen that the cruising speed under the sinusoidal pattern is 12.5% higher. This is because it is smoother and thus, the resulting thrust has no jittering. Therefore, the sinusoidal pattern is used in the subsequent experiment.

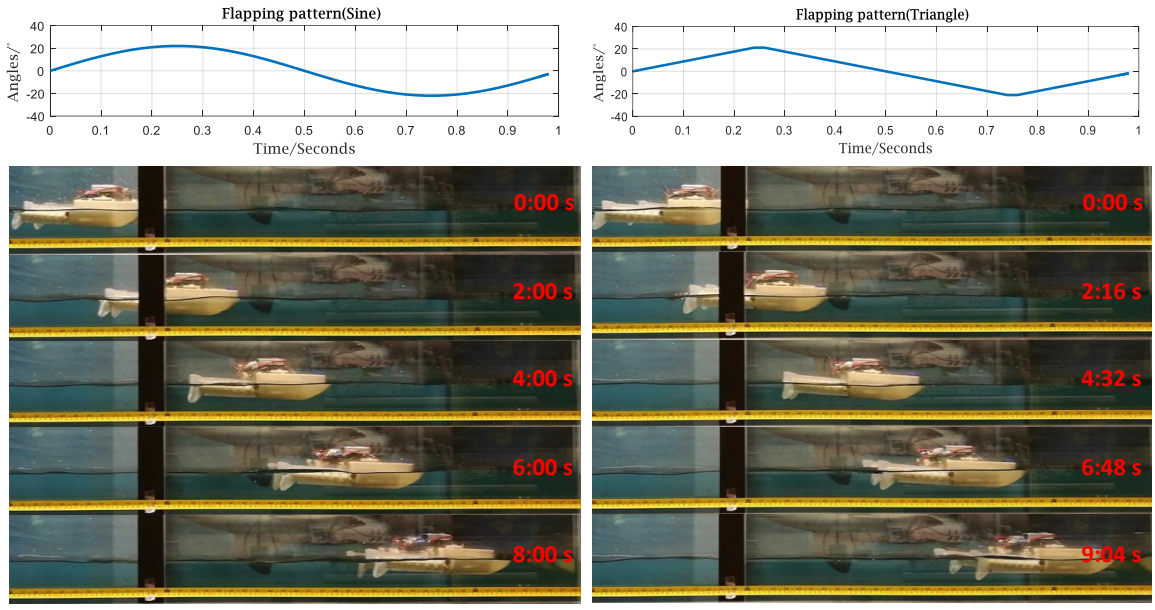

Fig. 8: Cruising performance tests: (a) sinusoidal pattern, (b) triangle pattern.

The second experiment is aimed to test turning performances under different turning modes. The results are shown in Tab.1. In all these experiments, the flapping frequency is 0.5Hz and the flapping amplitude is 90°. The turning radiuses of turning mode 1, 2, 3 are 800mm (2.3 body length), 180mm (0.517 body length), 300mm (0.862 body length), respectively, and the turning speeds are 4.2 °/s, 10.5°/s, 13.9°/s, from which it is seen that mode 2 has the minimum turning radius and mode 3 has the fastest turning speed.

Turning modes	*Turning radius*	*Turning speed*
Mode 1	800mm(2.300BL)	4.2 °/s
Mode 2	180mm(0.517BL)	10.5 °/s
Mode 3	300mm(0.862BL)	13.9 °/s

Tab. 1: Turning performances in different turning modes.

In the third experiment, the target of the boat is to track a circular white ball, and the results are shown in Fig. 9 and Fig.10. In the first 2 seconds, the target is found at right of the boat. As a result, left propulsive tail oscillates more intensively than the right tail to generate a torque to modify the orientation of the boat. Because the boat is subject to time delay, there will be some overshoot of the orientation modification. After the first two seconds, the right tail oscillates in larger amplitude to overcome the overshoot. Finally, the double-hull boat reaches the target successfully around the 10th second. The duty cycle variations of the two servomotors are shown in Fig.10. The magnitude of the duty cycle corresponds to the flapping amplitude of the propeller. A number of similar experiments have been performed and the boat is always capable of reaching the target.

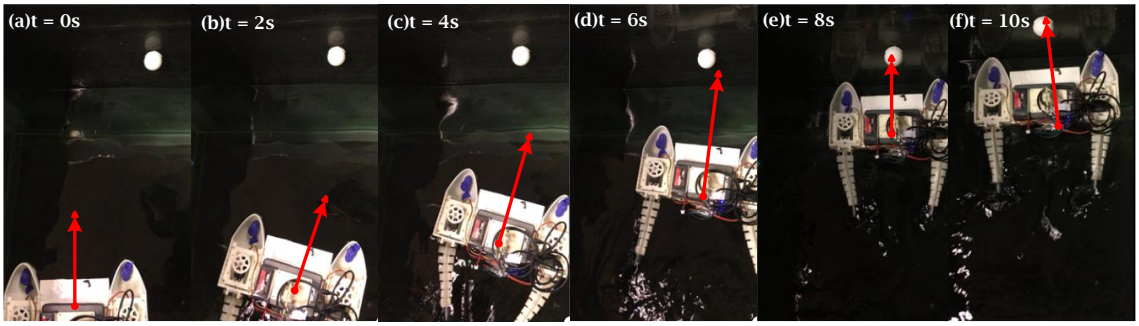

Fig. 9: Target tracking.

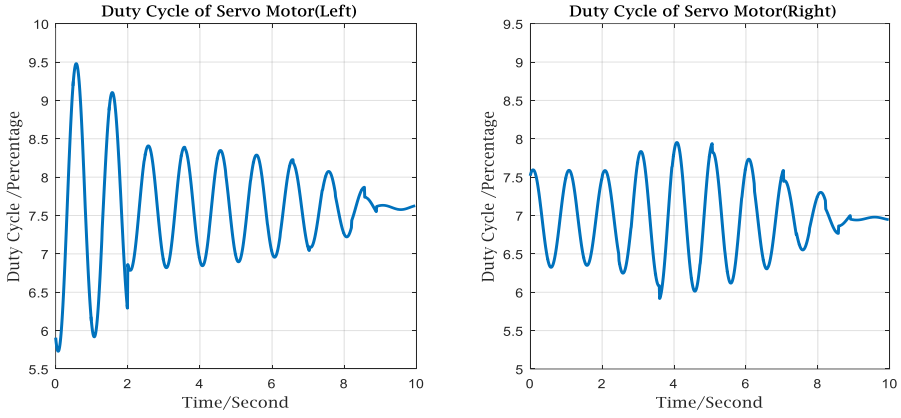

Fig. 10: Control signals of servo motors.

Conclusions:

This paper presents a biomimetic flapping based double-hull boat with a vision-based target tracking system. Based on the discussions above, following conclusions can be drawn:

(a) The boat can reach a speed of 0.314 BL / second, and turn with a minimum turning radius of 0.517 BL.

(b) Upon identifying the floating target, the boat can automatically adjust its moving direction to approach the target. Testing results indicated that the boat can always track the target when it is within its view.

In the future, a number of further developments will be carried out. Firstly, a rotational platform will be added onto the camera to increase the view of the camera. Secondly, the control algorithm will be optimized to maximize the tracking speed. Thirdly, the ability of obstacle avoidance will be added laying the foundation for autonomous navigation. Finally, by taking the advantages of the double-hull boat (small turning radius and capability of obstacle avoidance), advanced features such as parallel parking of boat will be investigated, which will help wharf management.

References:

[1] Alvarado, Y.; Valdivia, P.; Kamal, Y.-T.: Soft-Body Robot Fish, Robot Fish, Springer Berlin Heidelberg, 2015, 161-191. http://dx.doi.org/10.1007/978-3-662-46870-8_6

[2] International Chamber of shipping 2017 annual review. Available at: http://www.ics-shipping.org/docs/default-source/ICS-Annual-Review-2017/ics-annual-review-2017.pdf

[3] Li, Z.; Du, R.-X.: Wire-Driven Robot Fish, Robot Fish, Springer Berlin Heidelberg, 2015, 51-92. http://dx.doi.org/10.1007/978-3-662-46870-8_3

[4] Li, Z.; Du, R.-X.: A novel double-hull boat with biomimetic wire-driven flapping propulsors, 2014 IEEE International Conference on Robotics and Automation (ICRA), IEEE, 2014, http://dx.doi.org/10.1109/ICRA.2014.6907201
[5] Xie, G.-M.; Wang, L.; Hu, Y.-H.: Multiple Autonomous Robotic Fish Collaboration, Robot Fish, Springer Berlin Heidelberg, 2015, 315-357. http://dx.doi.org/10.1007/978-3-662-46870-8_11
[6] Yu, J.-Z.; Tan, M.: Design and Control of a Multi-joint Robotic Fish, Robot Fish, Springer Berlin Heidelberg, 2015,93-117. http://dx.doi.org/10.1007/978-3-662-46870-8_4